

# Integration and Comparison of Brain Functional and Structural Connectivity Maps

D. C. Zhu<sup>1</sup>, and S. Majumdar<sup>2</sup>

<sup>1</sup>Psychology and Radiology, Michigan State University, East Lansing, MI, United States, <sup>2</sup>Electrical and Computer Engineering, Michigan State University, East Lansing, MI, United States

## Introduction

Resting-state fMRI allows the testing of brain functional connectivity (1). Diffusion tensor imaging (DTI) fiber tracking allows the evaluation of structural connection between cortical regions (2). Often there is a need to integrate them together to understand the networks of brain activity, to compare their advantages and disadvantages, and to evaluate potential applications (3). In this work, we combined the functional and structural connectivity analyses based on common seed regions. The correlation coefficient was used to estimate the strength of the functional connectivity. The normalized connectivity distribution was used to estimate the strength of the structural connectivity. These choices allow the integration in both individual subject and group analyses. The integration demonstrates potential interpretation issues and also shows that functional connectivity might be a more sensitive and robust technique in understanding the connectivity between cortical regions.

## Methods

Six healthy adults (age 18-28, 2 male) were scanned on a GE 3T Signa® HDx MR scanner (GE Healthcare, Waukesha, WI) with an 8-channel head coil. For each subject, a seven-minute resting-state fMRI EPI dataset was collected first with the following parameter: 36 contiguous 3-mm axial slices in an interleaved order, TE = 27.7 ms, TR = 2500 ms, flip angle = 80°, FOV = 22 cm, matrix size = 64 × 64, ramp sampling, and with the first four data points discarded. The subject was instructed to relax and close his/her eyes during the fMRI scan. After the fMRI scan, T<sub>2</sub> and diffusion-weighted images for DTI were acquired with a dual spin echo EPI sequence with the following parameters: 48 contiguous 2.4-mm axial slices, TR = 13.7 s, TE = 75 ms, matrix size = 128 × 128, FOV = 22 cm × 22 cm, NEX = 2, parallel imaging acceleration factor = 2, b = 1000 s/mm<sup>2</sup>, and scan time = 12 min 20 s. A DTI sequence with a higher resolution but a reduced coverage was repeated with the modification of the following parameters: 43 contiguous 1.7-mm axial slices, TR = 11 s, FOV = 21 cm × 21 cm, and scan time = 12 min 20 s. T<sub>1</sub>-weighted high-resolution volumetric images were also collected.

Seed regions published in the paper by Andrews-Hanna et al. (4) were selected to evaluate the integration of the analyses: left middle temporal gyrus (LMTG) (L45, P67, S26), left posterior cingulate/retrosplenial cortex (pC/rsp) (L1, P50, S26), right cuneus (R19, P95, S2), left cuneus (L19, P95, S2) and right superior parietal lobule (RSPL) (R23, P63, S50). Each seed region was a sphere with the center at the corresponding Talairach coordinate indicated and with a radius of 6 mm.

Resting-state fMRI analysis was carried in AFNI (5). Slice-timing correction and motion correction were first applied. Then the baseline, linear and quadratic trends of the data, and the potentially motion-introduced artifacts were removed. The brain global mean signal change was modeled as the physiological noise assuming that the physiological noise affected the brain globally. This noise was modeled in the correlation analysis. This correlation analysis was done on every voxel of the brain against the time course from the average signal within the seed region. For each subject, the functionally connected regions were identified based on the voxel-based *P* value < 10<sup>-5</sup>.

The DTI datasets were processed with the Diffusion Toolbox in FSL software package (6), including the correction of eddy-current distortion and motion on the raw image data. Bayesian Estimation of Diffusion Parameters Obtained using Sampling Techniques (BEDPOST) (7) was applied. The probabilistic tractography (PROBTRACKX) within FSL was then applied to each seed region to calculate the corresponding connectivity distributions. The connectivity distributions were then normalized by the total number of generated tracts from the seed region. If the normalized connectivity distribution > 2 × 10<sup>-5</sup>, the voxel was considered a part of the connected fiber structure with respect to the seed region.

For each seed region in each subject, the functional and structural connections were then integrated together by a bitmap coding technique, specifically, “1” for functional connection, “2” for structural connection, and “3” for the coexistence of both. They can be color-coded for visualization. For each seed-region based group analysis, the mean correlation coefficient (threshold > 0.2) and the mean normalized connectivity distribution (threshold > 10<sup>-4</sup>) of the six subjects were integrated together similarly as in the individual subject but in the Talairach space.

## Results and Discussion

The integration for the functional and structural connectivity is demonstrated in a sample case (Fig. 1(a)) and in group analysis (Fig. 1(b)). Functional connected regions are expected to be connected together in structure. However, this relationship was often only found at the neighborhood of the seed regions in this study. As shown in Fig. 1(a), bilateral functional connection was seen in both single subject and group analyses as expected, but structural connection could not be identified with confidence to show across hemisphere between two functionally connected regions. In another situation as shown in Fig. 1(b), when regions are functional connected together in distant anatomical ranges, the fiber connection often fails to reach these functionally connected regions. Overall, besides the area surrounding the seed regions, the direct matches between the fibers and the respective functional regions were not obvious. This issue was seen in both DTI protocols. These mismatches could be due to multiple causes: (1) Functional connected regions might be linked by multiple neurons, and thus require multiple seed regions for fiber tracking. This would require human interpretation of the new seed regions and likely leads to bias. (2) Structurally connected regions do not mean that they are functionally connected. (3) Successful fiber tracking requires good image signal-to-noise ratio, good resolution, and a full coverage of the tracks of interest. This demands optimized pulse sequences and protocols and a long scan time. Therefore, functional connectivity might be a more sensitive and robust technique in understanding the connectivity between cortical regions.

## References

1. Fox MD, Raichle ME. Nat Rev Neurosci. 2007; 8:700-711.
2. Le Bihan D, Mangin JF, Poupon C, Clark CA, Pappata S, Molko N, Chabriat H. J Magn Reson Imaging. 2001;13:534-546.
3. Greicius MD, Supekar K, Menon V, Dougherty RF. Cereb Cortex. (In Press.)
4. Andrews-Hanna JR, Snyder AZ, Vincent JL, Lustig C, Head D, Raichle ME, Buckner RL. Neuron. 2007;56:924-935.
5. Cox RW. Comput Biomed Res 1996;29:162-173.
6. Smith SM, Jenkinson M, Woolrich MW, et al. 2004. Neuroimage 2004;23:S208-219.
7. Behrens TE, Berg HJ, Jbabdi S, Rushworth MF, Woolrich MW. NeuroImage 2007, 34:144-155.

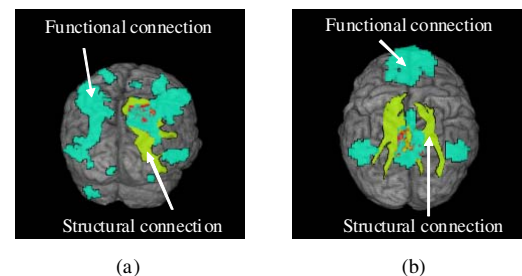


Fig. 1. The integration of the functional and structural connections is shown. (a) The single-subject analyses shown were carried with the right SPL as the seed region. (b) The whole-group analyses shown were carried with the pC/rsp as the seed region. Red = coexistence of the two connection types, blue = functional connection only, green = structural connection only.